Electronic Supplementary Material (ESI) for Materials Horizons.
This journal is © The Royal Society of Chemistry 2021

Supplementary Materials for

Breaking through the "3.0 eV wall" of energy band gap in mid-infrared nonlinear optical rare earth chalcogenides by charge-transfer engineering

Dajiang Mei[a,c]*, Wangzhu Cao[a], Naizheng Wang[bd], Xingxing Jiang[b]*, Jun Zhao[a], Weikang Wang[a], Junhui Dang[a], Shiyan Zhang[a], Yuandong Wu[a], Pinhua Rao[a] and Zheshuai Lin[b,d]*

[a]College of Chemistry and Chemical Engineering, Shanghai University of Engineering Science, Shanghai 201620, China.

Email: meidajiang718@pku.edu.cn

[b]Technical Institute of Physics and Chemistry, Chinese Academy of Sciences, Beijing 100190, China

Email: xxjiang@mail.ipc.ac.cn, zslin@mail.ipc.ac.cn

[c]State Key Laboratory of Crystal Materials and Institute of Crystal Materials, Shandong University, Jinan, 250100, China

[d]University of Chinese Academy of Sciences, Beijing 100049, China

Experimental and Computational Method.

Fig. S1. EDS analyses of $KYGeS_4$.

Fig. S2. The difference trace between experimental and calculated XRD data of $KYGeS_4$.

Fig. S3. Powder XRD pattern of $AgGaS_2$.

Fig. S4. SHG intensity of $KYGeS_4$ plotted against particle size.

Fig. S5. The calculated band structure of (a) $KYGeS_4$ and (b) Y_2S_3.

Fig. S6. The calculated band structure of GeS_2.

Fig. S7. Partial density of states projected on respective atoms in GeS_2.

Fig. S8. Optical reflection spectrum of $KYGeS_4$ with the plot of K/S versus E.

Fig. S9. SHG effect superposition of $[GeS_4]$ tetrahedra.

Fig. S10. Distorted $[YS_7]$ polyhedra arrangement.

Fig. S11. Calculated refractive index of $KYGeS_4$.

Table S1. Crystallographic data and details of structure refinement for $KYGeS_4$.

Table S2. Selected bond lengths (Å) and angles (deg) of $KYGeS_4$.

Table S3. The NLO data of the reported MIR NLO rare earth sulfides.

Experimental and Computational Method

Synthesis

K_2S_3 (K_2S_3 were prepared by liquid ammonia method), Y powder (aladdin, 99.9%), Ge powder (aladdin, 99.999%), S powder (Sinopharm Chemical Reagent, 99.99%) were used as raw materials and put in a glove box filled with argon (the content of water and oxygen were both less than 0.1 ppm). These raw materials were mixed homogeneously and then sealed in a quartz tube under vacuum condition. The quartz tube was slowly heated to 1073 K for 20 h and held for 10 h in a programmed furnace. Powder samples were obtained after this procedure.

Single crystal growth

Mixture of the raw materials were sealed in a carbon-coated quartz tube. The tube was heated to 1123 K for 20 h and held for 4 days, then slowly cooled to 573 K at a rate of 4 K/h. After the cooling, the $KYGeS_4$ crystals were obtained (Crystal size: 0.1-0.2 mm).

Energy dispersive X-ray spectrometer

Energy dispersive X-ray spectrometer (EDS) testing was performed on Oxford NT 80 instrument, and the result showed that the atomic ratio of K, Y, Ge and S in $KYGeS_4$ are 13.46%, 13.78%, 14.64% and 58.12% (Fig. S1).

Powder X-ray diffraction

X-ray diffractometer equipped with Cu Kα radiation was used to collect the diffraction data of $KYGeS_4$ and $AgGaS_2$ at room temperature. The scanning range of 2θ is 10-70°. The difference trace between their experimental and calculated XRD data of $KYGeS_4$ has been provided by using the GSAS program package (Fig. S2).[1] The diffraction peaks are in good consistence with the simulated result, confirming the high purity of as-obtained $KYGeS_4$.

Determination of crystal structure

High-quality single crystal was firstly selected under electron microscope. Crystal structure data of $KYGeS_4$ was collected and analyzed by using a Bruker single crystal diffractometer equipped with graphite-monochromatized Mo Kα radiation (λ =

0.71073 Å). It should be noted that the voltage and current of the X-ray tube were set at 50 kV and 30 mA respectively. SHELXTL[2,3] software package was used to solve the crystal structure directly and the matrix least square method was used to refine the structure of $KYGeS_4$.

UV-Vis diffuse reflectance spectroscopy analysis

The diffuse reflectance spectra of the $KYGeS_4$ powder were tested by Shimadzu UV-3600 spectrophotometer with a test range of 200-1500 nm. $BaSO_4$ powder was chosen to be the 100% reflectance standard.

Laser damage threshold measurement

As the previous references[4-6] described, the laser damage threshold of $KYGeS_4$ powder was measured by pulsed YAG laser.[6] The wavelength, pulse width and pulse repetition frequency were set at 1064 nm, 10 ns, 10 Hz, respectively.[5] $AgGaS_2$ powder with the similar particle size was chosen as a reference material.

Second harmonic generation measurement

The modified Kurtz-Perry method was used to assess the SHG response of samples,[7] the laser source was a 1.06 μm Q-switched Nd: YAG.

First-principles calculations

The first-principles calculation was performed by CASTEP,[8] a total energy package based on the plane-wave pseudopotential density functional theory (DFT).[9,10] The exchange-correlation function was described by screened-exchange local density approximation (sX-LDA),[11] which has been verified to be able to accurately the band gap of semi-conductor materials.[12] The effective nucleus-electron interactions were modeled by the norm-conserving pseudopotentials for all element, with K $3s^23p^64s^1$, Y $4s^24p^64d^15s^2$, Ge $4s^24p^2$ and S $3s^23p^4$ treated as valence electrons,[13] which allow the employment of a relatively small plane-wave basis set without compromising the computational accuracy. The kinetic energy cutoff of 900 eV and intensive Monkhorst−Pack k-point meshes spanning less than 0.04/$Å^3$ were chosen.[14] Based on the calculated band structure, the imaginary part of the dielectric function was calculated and the real part of the dielectric function, *i.e.*, refractive index, was determined by Kramers–Kronig transformation.[15] The second-harmonic generation

(SHG) coefficient was calculated using the program developed by our group.[16,17] To analyze the contribution of the relevant groups to the optical properties, a real-space atom-cutting technique is employed, where the contribution of ion *A*, $\chi(A)$, to the optical coefficients is acquired by excluding all the atoms from the original wave function except *A*, i.e.: $\chi(A) = \chi$(all atoms excluded except *A*) .[16] The structural model of Y_2S_3 used in the calculation is determined by T. Schleid,[18] and that.of GeS_2 is experimentally determined by VG. Dittmar *et al*.[19]

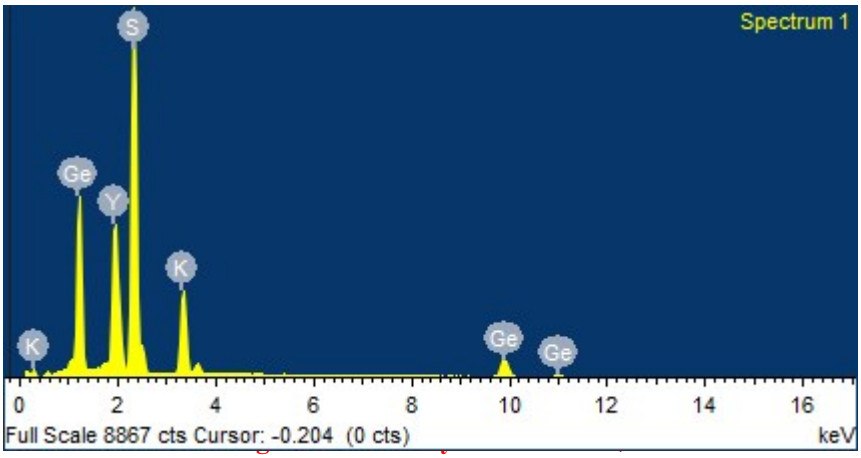

Fig. S1. EDS analyses of $KYGeS_4$

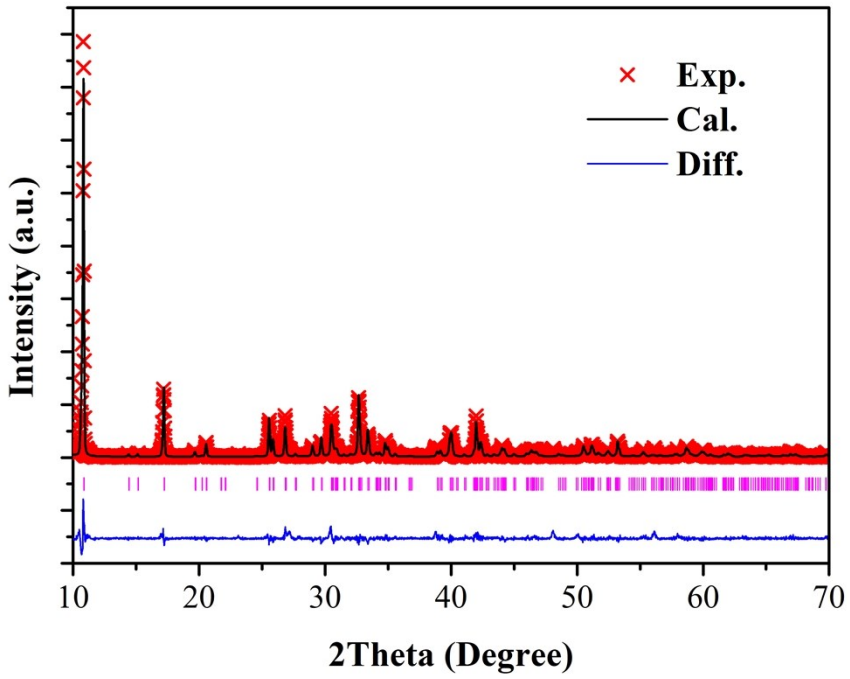

Fig. S2. The difference trace between experimental and calculated XRD data of $KYGeS_4$.

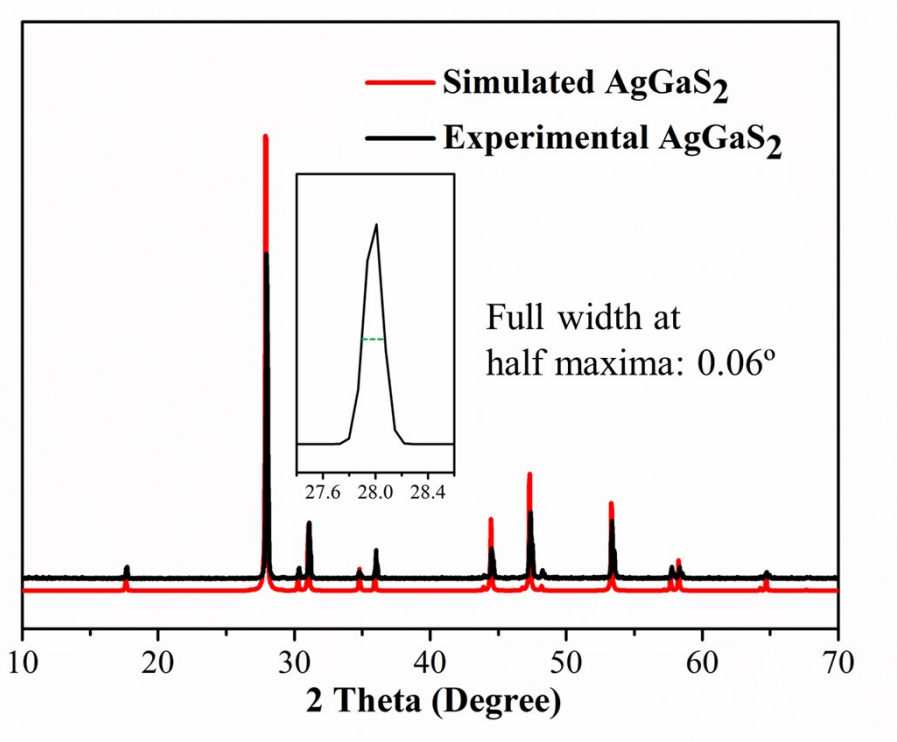

Fig. S3. Powder XRD pattern of $AgGaS_2$.

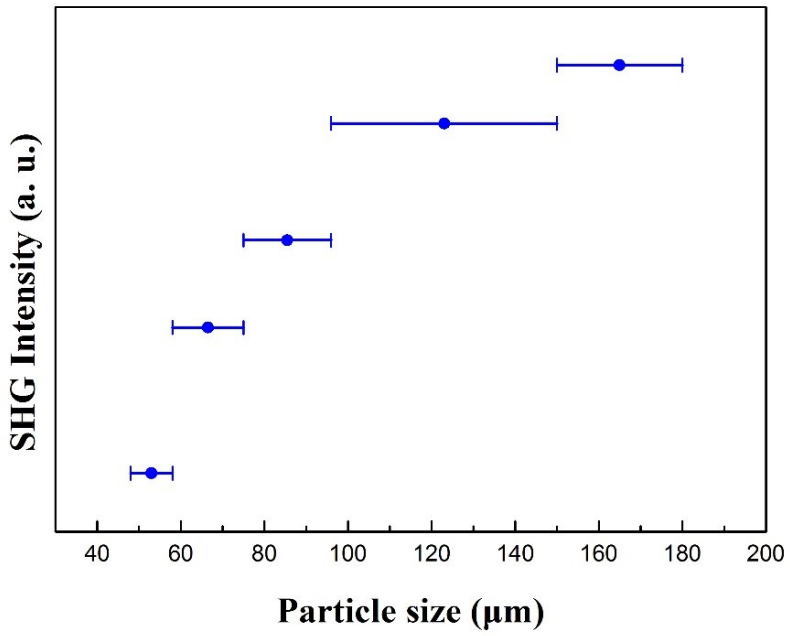

Fig. S4. SHG intensity of $KYGeS_4$ plotted against particle size.

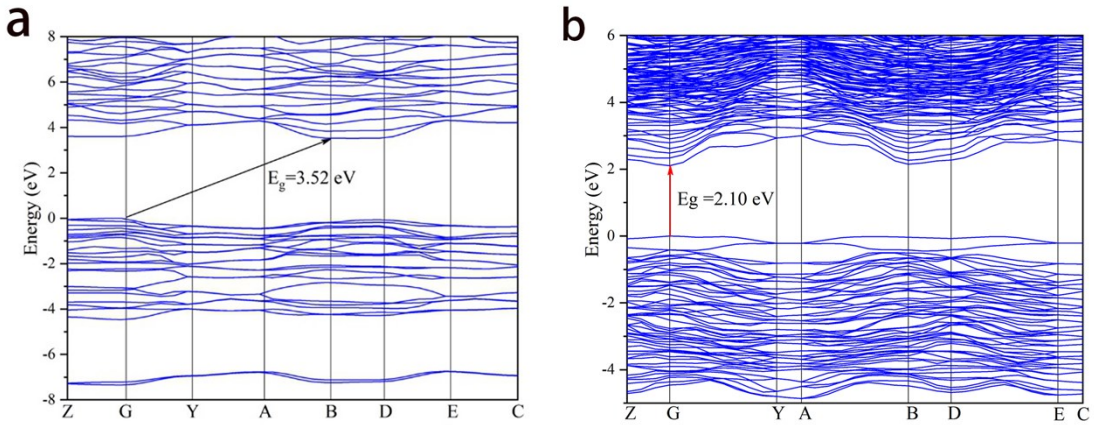

Fig. S5. The calculated band structure of (**a**) $KYGeS_4$ and (**b**) Y_2S_3.

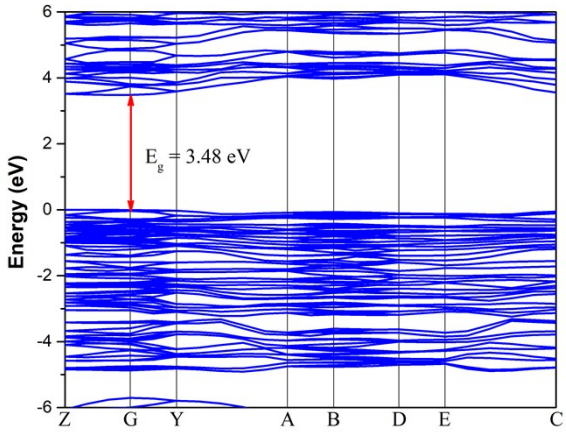

Fig. S6. The calculated band structure of GeS_2.

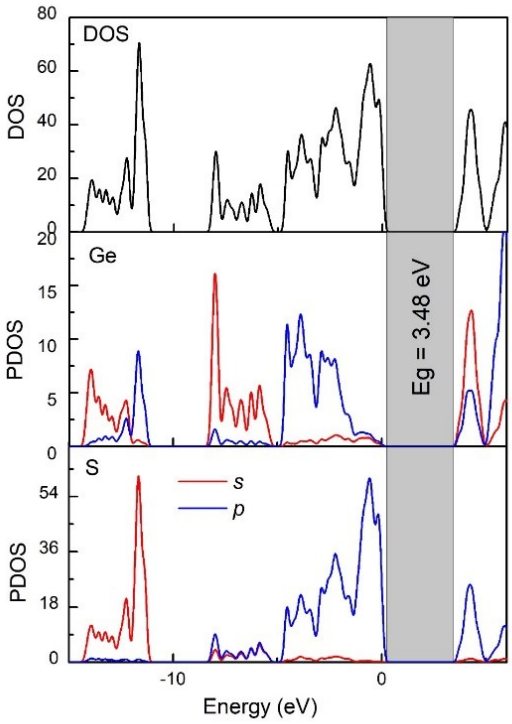

Fig. S7. Partial density of states projected on respective atoms in GeS_2.

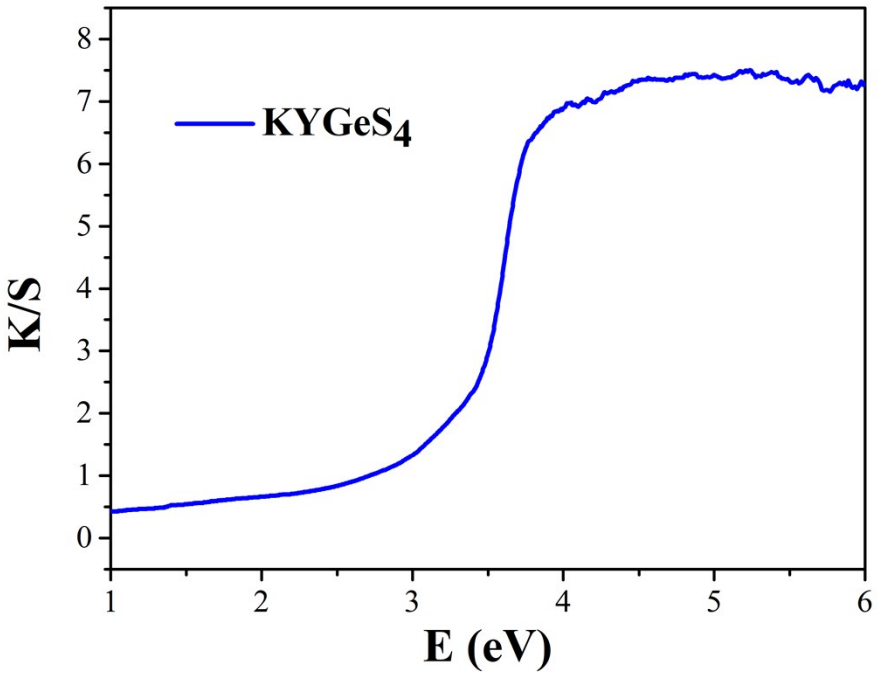

Fig. S8. Optical reflection spectrum of $KYGeS_4$ with the plot of K/S versus E.

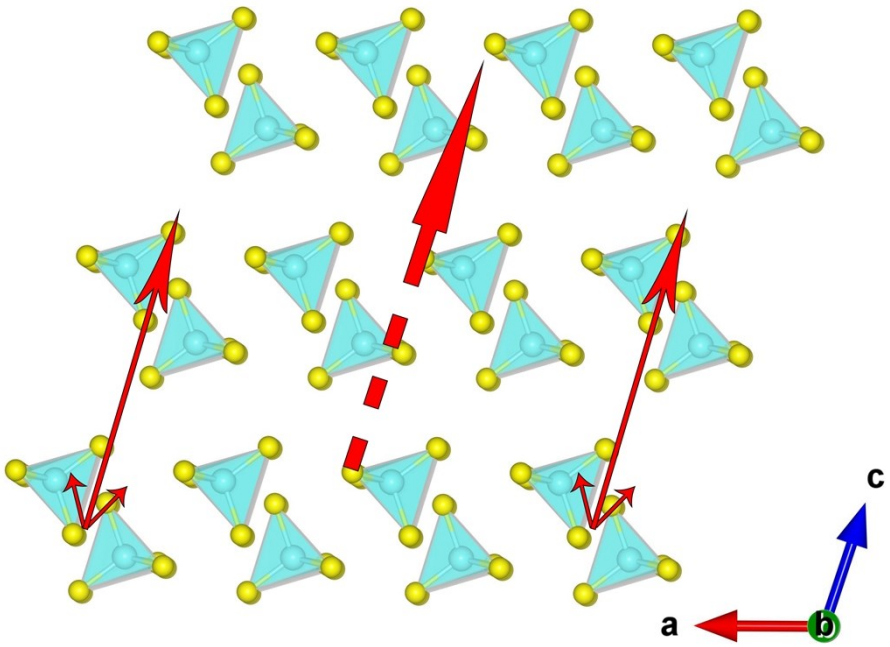

Fig. S9. SHG effect superposition of [GeS_4] tetrahedra.

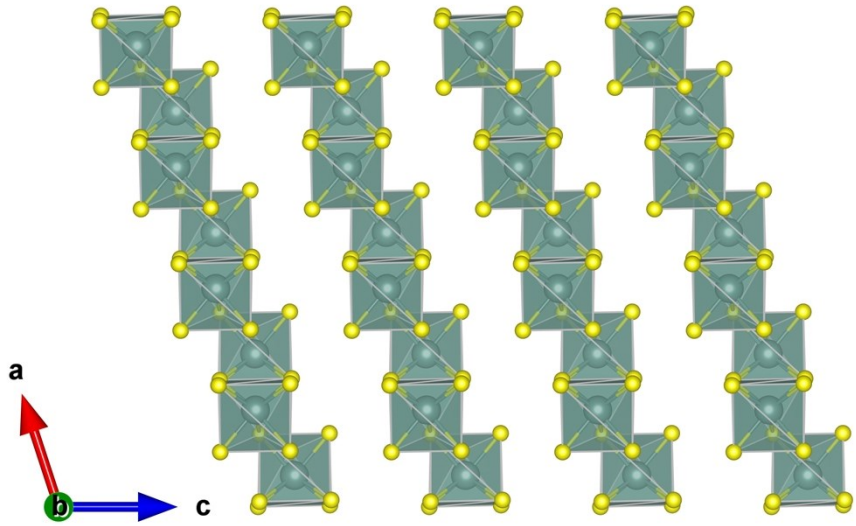

Fig. S10. Distorted [YS_7] polyhedra arrangement.

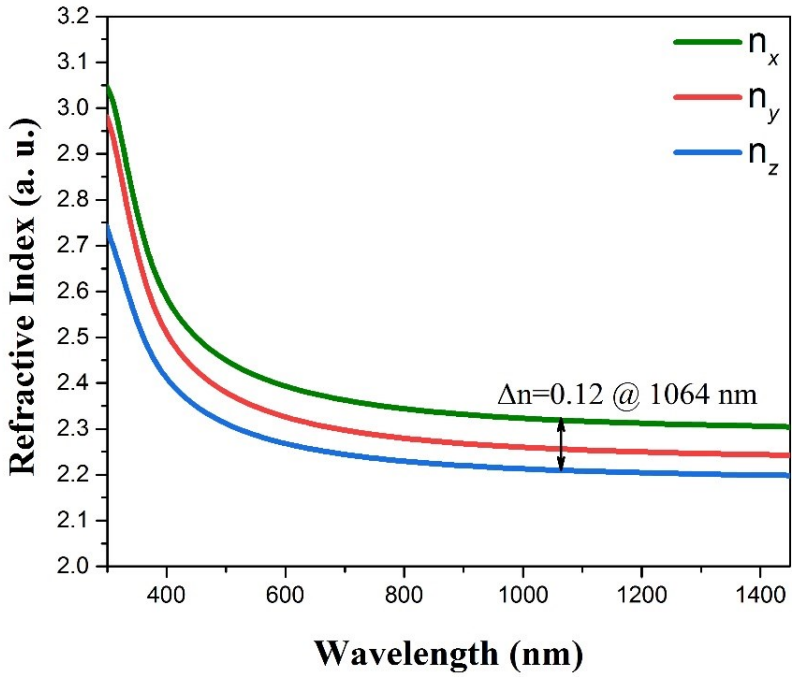

Fig. S11. Calculated refractive index of $KYGeS_4$.

Table S1. Crystallographic data and details of the structure refinement for $KYGeS_4$.

Empirical formula	$KYGeS_4$
Formula weight	328.84
a (Å)	6.428(6)
b (Å)	6.641(6)
c (Å)	8.612(8)
α (°)	90
β (°)	108.07
γ (°)	90
Volume（$Å^3$）	349.5(6)
Z	2
Crystal system	monoclinic
Space group	$P2_1$
Index ranges	$-7 \leq h \leq 7$
	$-6 \leq k \leq 7$
	$-10 \leq l \leq 9$
Theta range	2.488 – 25.017
Calculated density（g/cm^3）	3.125
Absorption coefficient（mm^{-1}）	14.226
Final R indices [I>2sigma(I)]	$R_1 = 0.0152$, $wR_2 = 0.0341$
R indices (all data)	$R_1 = 0.0158$, $wR_2 = 0.0339$

Weight = 1 / [sigma^2(F_o^2) + (0.0220 * P) ^2 + 84.95 * P] where P = (Max (Fo^2, 0) + 2 * F_c^2) / 3

Table S2. Selected bond lengths (Å) and angles (deg) of $KYGeS_4$.

Bond distance	(Å)	Bond distance	(Å)
Ge1-S1	2.170(2)	Y1-S2	2.950(3)
Ge1-S2	2.201(2)	Y1-S3	2.843(2)
Ge1-S3	2.202(2)	Y1-S3	2.876(2)
Ge1-S4	2.205(2)	Y1-S4	2.814(2)
Y1-S1	2.768(2)	Y1-S4	2.807(2)
Y1-S2	2.776(2)		
Bond angle	**(deg.)**	**Bond angle**	**(deg.)**
S1-Ge1-S3	115.72(7)	S3-Y1-S2	143.02(5)
S1-Ge1-S4	113.51(6)	S4-Y1-S3	70.62(7)
S1-Ge1-S2	108.05(8)	S4-Y1-S3	73.29(7)
S3-Ge1-S4	100.66(9)	S4-Y1-S3	79.54(7)
S2-Ge1-S3	103.16(6)	S4-Y1-S3	78.84(8)
S2-Ge1-S4	115.38(6)	S4-Y1-S4	119.71(6)
S1-Y1-S3	151.71(5)	S4-Y1-S2	76.44(7)
S1-Y1-S3	82.10(7)	S4-Y1-S2	135.78(5)
S1-Y1-S4	92.84(8)	S2-Y1-S3	97.59(7)
S1-Y1-S4	134.70(6)	S2-Y1-S3	125.16(6)
S1-Y1-S2	79.29(8)	S2-Y1-S4	78.95(7)
S1-Y1-S2	78.66(5)	S2-Y1-S4	157.86(5)
S3-Y1-S3	120.59(6)	S2-Y1-S2	81.71(5)
S3-Y1-S2	73.08(6)		

Table S3. The NLO data of the reported MIR NLO rare earth sulfides. The compounds with quasi-rigid *p*-block element tetra-coordinated groups contain the rare earth cations La^{3+}, Sm^{3+} or Eu^{2+}. For Sm^{3+} and Eu^{2+} the 4*f* orbitals are not fully or half occupied, and in these compounds the energy band gaps are predominantly determined by the *f*-*f* electronic transition within the rare earth cations,[27,28] which are hardly modified by the charge-transfer from quasi-rigid groups. On the other hand, La belongs to the sixth period in the period table of elements, and its radius are larger than that of Y (in fifth period). Since the band gap of a compound decreases as the radius of contained element increases,[31] the La containing sulfides certainly possess narrower band gaps than $KYGeS_4$, even though the quasi-rigid [GeS_4] and [SiS_4] groups could induce the same charge-transfer in the former compounds as in the latter.

Compound	Band gap	SHG	Ref
$La_8Sb_2S_{15}$	2.30 eV	1.2 × AGS	20
La_4InSbS_9	2.07 eV	1.5 × AGS	21
Sm_4InSbS_9	2.13 eV	0.75 ×AGS	22
Sm_4GaSbS_9	2.23 eV	3.8 × AGS	23
Gd_4GaSbS_9	2.41 eV	0.8 × AGS	23
Ba_2InYSe_5	2.31 eV	1 × AGSe	24
$La_6Ga_2GeS_{14}$	2.54 eV	4.8 × AGS	25
$La_6In_2GeS_{14}$	2.61 eV	1.8 × AGS	25
$LiSm_3SiS_7$	2.83 eV	1.5 × AGS	26
$Eu_2Ga_2GeS_7$	2.30 eV	1.6 × AGS	27
$EuCdGeS_4$	2.5 eV	2.6 × AGS	28
$EuCdGeSe_4$	2.25 eV	3.8 × AGS	28
Y_3GaS_6	2.88 eV	0.5 × KTP	29
La_2CuSbS_5	2.06 eV	0.5 × AGS	30

References

1. A. C. Larson and R. B. Von Dreele, General Structure Analysis System (GSAS), Los Alamos National Laboratory Report LAUR 86-748 (1994).
2. G. M. Sheldrick, *Acta Cryst.*, 2008, A**64**, 112-122.
3. G. M. Sheldrick, *Acta Cryst*., 2015, C**71**, 3-8.
4. J. Zhao, D. J. Mei, Y. Yang, W. Z. Cao, C. Liu, Y. D. Wu and Z. S. Lin, *Inorg. Chem*., 2019, **58**, 15029-15033.
5. C. Liu, D. J. Mei, W. Z. Cao, Y. Yang, Y. D. Wu, G. B. Li and Z. S. Lin, *J. Mater. Chem. C*, 2019, **7**, 1146-1150.
6. G. M. Li, K. Wu, Q. Liu, Z. H. Yang and S. L. Pan, *J. Am. Chem. Soc.*, 2016, **138**, 7422-7428.
7. S. K. Kurtz and T. T. Perry, *J. Appl. Phys*., 1968, **39**, 3798-3813.
8. S. J. Clark, M. D. Segall, C. J. Pickard, P. J. Hasnip, M. I. J. Probert, K. Refson and M. C. Payne, *Z. Kristallogr*., 2005, **220**, 567-570.
9. W. Kohn and L. J. Sham, *Phys. Rev*., 1965, **140**, A1133- A1138.
10. M. C. Payne, M. P. Teter, D. C. Allan, T. A. Arias and J. D. Joannopoulos, *Rev. Mod. Phys*., 1992, **64**, 1045-1097.
11. R. Asahi, W. Mannstadt and A. J. Freeman, *Phys. Rev. B*, 1999, **59**, 7486-7492.
12. L. Kang, M. L. Zhou, J. Y. Yao, Z. S. Lin, Y. C. Wu and C. T. Chen, *J. Am. Chem. Soc*., 2015, **137**, 13049-13059.
13. D. R. Hamann, M. Schlüter and C. Chiang, *Phys. Rev. Lett.*, 1979, **43**, 1494-1497.
14. H. J. Monkhorst and J. D. Pack, *Phys. Rev. B*, 1976, **13**, 5188-5192.
15. E. D. Palik, *Academic: New York* 1985.
16. J. Lin, M. H. Lee, Z. P. Liu, C. T. Chen and C. J. Pickard, *Phys. Rev. B,* 1999, **60**, 13380-13389.
17. Z. S. Lin, X. X. Jiang, L. Kang, P. F. Gong, S. Y. Luo and M. H. Lee, *J. Phys. D: Appl. Phys*., 2014, **47**, 253001.
18. T. Schleid, *Eur. J. Solid State Inorg. Chem*., 1992, **29**, 1015-1028.
19. V. G. Dittmar and H. Schäfer, *Acta Cryst.*, 1975, **B31**, 2060-2064.
20. H. J. Zhao and L. J. Zhou, *Eur. J. Inorg. Chem*., 2015, 964-968.
21. H. J. Zhao, Y. F. Zhang and L. Chen, *J. Am. Chem. Soc*., 2012, **134**, 1993-1995.
22. H. J. Zhao, *Z. Anorg. Allg. Chem*., 2016, **642**, 56-59.
23. M. C. Chen, L. H. Li, Y. B. Chen and L. Chen, *J. Am. Chem. Soc*., 2011, **133**, 4617-4624.
24. W. L. Yin, K. Feng, W. D. Wang, Y. G. Shi, W. Y. Hao, J. Y. Yao and Y. C. Wu, *Inorg. Chem*., 2012, **51**, 6860-6867.
25. Y. F. Shi, Y. K. Chen, M. C. Chen, L. M. Wu, H. Lin, L. J. Zhou and L. Chen, *Chem. Mater*., 2015, **27**, 1876-1884.
26. N. Zhen, L. Y. Nian, G. M. Li, K. Wu and S. L. Pan. *Crystals*, 2016, **6**, 121.
27. M. C. Chen, P. Li, L. J. Zhou, L. H. Li and L. Chen, *Inorg. Chem*., 2011, **50**, 12402-12404.
28. W. H. Xing, N. Z. Wang, Y. W. Guo, Z. Li, J. Tang, K. J. Kang, W. L. Yin, Z. S. Lin, J. Y. Yao and B. Kang, *Dalton. Trans*., 2019, **48**, 17620-17625.
29. M. J. Zhang, B. X. Li, B. W. Liu, Y. H. Fan, X. G. Li, H. Y. Zeng and G. C. Guo*, Dalton Trans*., 2013, **42**, 14223-14229.
30. H. Lin, Y. Y. Li, M. Y. Li, Z. J. Ma, L. M. Wu, X. T. Wu and Q. L. Zhu, *J. Mater. Chem. C,* 2019, **7**, 4638-4643.
31. L. M. Sharaf El-Deen, M. S. Al Salhi and M. M. Elkholy, *J. Alloy. Compound.*, 2008, **465**, 333-

339.